Progress In Electromagnetics Research C, Vol. 58, 79–87, 2015

Design and Implementation of Connected Antenna Array for Ultra-Wideband Applications

Yanfang Wang[1], Fuguo Zhu[2, 3, 4, *], and Steven Gao[3]

Abstract—An integrated eight-element antenna array has been proposed for ultra-wideband (UWB) applications. It consists of eight UWB antenna elements and an eight-way binary-tree modified Wilkinson power divider. Any two adjacent elements in the array are connected to each other and share a common side, thus leading to a connected antenna array. Moreover, this arrangement can be utilized to avoid grating lobe level at higher frequencies. Each antenna element comprises a square ring patch and is excited by a tapered balun to achieve low cross-polarization levels. In order to validate the design, a prototype has been fabricated and measured. Both simulated and measured results confirm that the proposed integrated antenna array achieves a good performance of a reflection coefficient below −10 dB from 2.9 GHz to 10.8 GHz, including stable radiation patterns with low side lobe and cross-polarization levels, thus the antenna is promising for applications in UWB imaging systems.

1. INTRODUCTION

Since the allocation of the frequency band from 3.1 GHz to 10.6 GHz by the Federal Communications Commission (FCC) in 2002, UWB has been a promising technology for UWB imaging radar applications due to its large bandwidth, low power consumption, and resistance to the multipath phenomenon [1]. This means that the UWB radar can identify target classes and types with a high resolution. As a key component of UWB systems, various UWB antennas have been proposed in the literature. Compared with single antenna element, antenna arrays are widely used in RF systems to control radiation patterns. Array pattern can be scanned or steered in angular space through electronics control of the element excitation. Moreover, the gain of the antenna can be enhanced by increasing the number of the elements in the array.

A preliminary study of utilizing wavelength-scaled array concept to achieve UWB performance has been explained in [2]. The broad bandwidth is obtained using scaled elements of different sizes. However, it requires a large size as more than one element is required to achieve a broad bandwidth. Compared with the wavelength-scaled array concept, compact size can be achieved by selecting a UWB antenna element to compose the UWB antenna array. Among various UWB antennas [3–12], planar UWB monopole [6–8] and tapered slot antenna [9–12] are widely used in UWB antenna array designs, as they have characteristics of broad bandwidth, simple structure and easy fabrication.

UWB monopole array [6, 7] has a wide frequency band but bidirectional radiation patterns and low antenna gain. In addition, the side lobe levels are high at higher frequencies due to the higher-mode. In comparison with UWB monopole array, tapered slot antenna array can achieve a wide frequency band with stable directional patterns. Furthermore, connected tapered slot antenna array has been proposed in [11, 12]. The investigation in [11] shows that the mutual coupling in the highly coupled array is essential and has good effect in wideband antenna array design. The design can operate from 1.6 to

Received 17 May 2015, Accepted 22 June 2015, Scheduled 8 July 2015

* Corresponding author: Fuguo Zhu (zhu.fuguo@hotmail.com).

[1] College of Computer and Information, Hohai University, Nanjing 211100, China. [2] Science and Technology on Antenna and Microwave Laboratory, Nanjing 210039, China. [3] School of Engineering and Digital Arts, University of Kent, Canterbury CT2 7NT, UK. [4] The 14th Research Institute, CETC, Nanjing 210039, China.

9 GHz and scan angle up to 45°. However, the antenna gain of the tapered slot antenna array in [12] increases significantly against frequency, indicating inconsistent antenna gain performance across the operating frequency band.

In this work, a novel UWB antenna element with a wide frequency band and directional radiation patterns is proposed. Eight antenna elements are connected to form an UWB array which is excited by an UWB power divider. To validate the design, a prototype has been fabricated and tested. Both simulated and measured results are shown and discussed in details.

2. UWB ANTENNA ELEMENT DESIGN

The design of the single antenna element started from our previous work in [13]. The proposed dual-polarized UWB patch antenna has a multi-layer structure which makes the fabrication very complicated. To ease the fabrication and keep the wide bandwidth, the radiating patch and feeding patch are on the same layer while a slot is embedded in the patch to enlarge the operating bandwidth [14]. However, this dual-polarized slot-loaded patch antenna has a large size which is not suitable for compact-size system applications. Figure 1 presents the configuration of the proposed UWB antenna element which features a compact size and fewer layers. Two L-shaped feeds are attached to a square ring patch with outer and inner lengths of W and l_1, respectively. Each L-shaped feed consists of a vertical trapezoidal patch with a height of H_2 and a horizontal rectangular patch with width and length of w_2 and l_2, respectively. The lengths of the top and bottom sides of the vertical trapezoidal patch are w_2 and w_3. The ground plane with a size of 70 mm × 70 mm is printed on the top layer of an FR4 substrate ($\varepsilon_2 = 4.55$, $h_2 = 0.8$ mm) and two identical microstrip lines with a length of l and a width of w are on the other side. Such arrangement can reduce the effect of the feeding network on the broadside radiation. A Rohacell foam of thickness $h_1 = 2$ mm is inserted between the ground plane and the bottom side of the vertical trapezoidal patch. The outer ends of the two microstrip lines are connected to the trapezoidal patches by two vias through via holes which are embedded in the ground plane. Good impedance matching across a wide frequency range can be obtained by selecting proper dimensions of the L-shaped

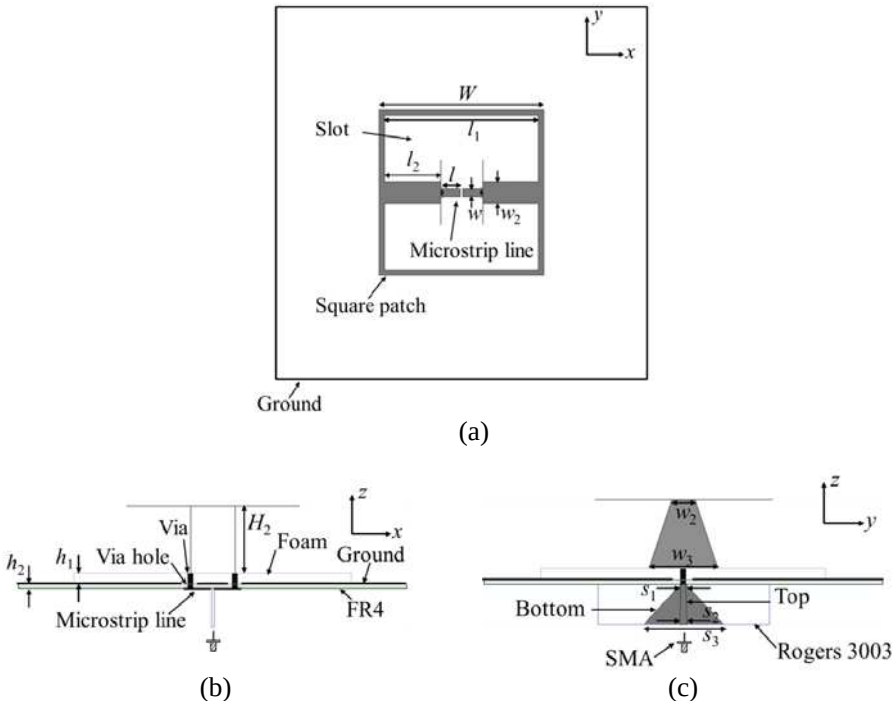

Figure 1. Geometry of the proposed single UWB antenna element. (a) Top view. (b) Front view. (c) Side view.

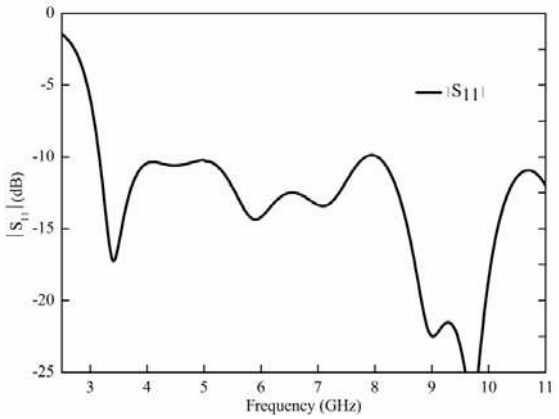

Figure 2. Simulated reflection coefficient of the UWB antenna element. Antenna dimensions: $W = 31\,\text{mm}$, $l_1 = 29\,\text{mm}$, $l_2 = 10.5\,\text{mm}$, $l = 4.5\,\text{mm}$, $w = 1.5\,\text{mm}$, $w_2 = 4\,\text{mm}$, $w_3 = 12\,\text{mm}$, $H_2 = 12\,\text{mm}$, $s_1 = 0.8\,\text{mm}$, $s_2 = 1.25\,\text{mm}$, and $s_3 = 14\,\text{mm}$.

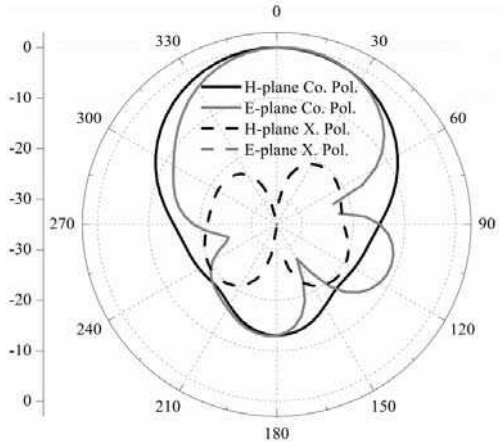

Figure 3. Simulated radiation patterns in two principal planes at 3 GHz.

feeds. In order to realize differential feed which can lead to low cross-polarization and high isolation, a simple tapered balun [15] is utilized to excite the antenna. As shown in Figure 1(c), the balun is printed on a Rogers 3003 substrate with size of $7\,\text{mm} \times 30\,\text{mm} \times 0.5\,\text{mm}$ and relative permittivity of 3.0, and perpendicularly placed to the surface of the grounded FR4 substrate. The top sides of the balun are connected to the inner ends of two microstrip lines on the grounded FR4 substrate while the bottom side is soldered to a $50\,\Omega$ SMA connector. It is worth mentioning that the gap between the inner ends of the two microstrip lines is the same as the thickness of the Rogers 3003 substrate for the balun. In practical applications, the polarization of the radiator is determined by the direction of the radiated E-field with respect to the ground. Suppose the radiator in Figure 1 is located parallel to the ground, then it can radiate horizontally polarized wave.

The simulation of the design has been carried out using HFSS 15.0 and the optimized values of corresponding dimensions are illustrated in Figure 2. The simulated results in terms of reflection coefficient and radiation patterns are shown in Figures 2 and 3 to describe the performance of the antenna. The side length of the ring patch is 31 mm which is around 0.3λ, 0.6λ and 0.9λ at 3, 6, and 9 GHz, respectively (λ is the wavelength in free space at each frequency). It is noted in Figure 2 that, the antenna achieves good impedance matching over a wide frequency range and the impedance bandwidth for $|S_{11}| \leq -10\,\text{dB}$ is from 3.1 to 11 GHz which covers the desired FCC UWB frequency band. Figure 3 presents the simulated normalized radiation pattern in two principal planes at 3 GHz. The boresight realized gain in simulation is found to be 6.77 dBi. As observed, it features broadside radiation and the cross-polarization levels are below $-20\,\text{dB}$ in both planes. The backward radiation level is less than $-12\,\text{dB}$. Due to the symmetrical geometry with respect to x-axis, the cross-polarization level in the E-plane is less than $-35\,\text{dB}$. The plotted curve has changed to a dot in the center of the figure.

3. EIGHT UWB ANTENNA ELEMENT ARRAY

Based on the analysis of the single UWB antenna element in the previous section, an eight-element array will be discussed in this section. Figure 4 presents the geometry of the connected array. To avoid grating lobes, the following condition should be satisfied [16],

$$d < \lambda/(1 + \sin(\theta)) \tag{1}$$

where λ is the wavelength of the highest frequency, θ is the angle between the scanning direction and the z-axis. Here, θ equals to 0 degree as the radiation is at boresight. As any two adjacent elements

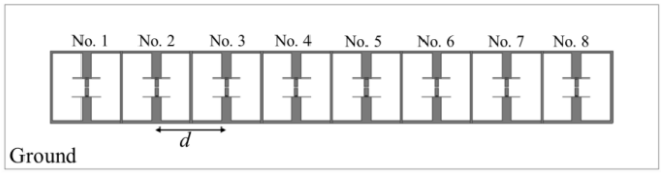

Figure 4. Array of eight connected UWB antenna elements.

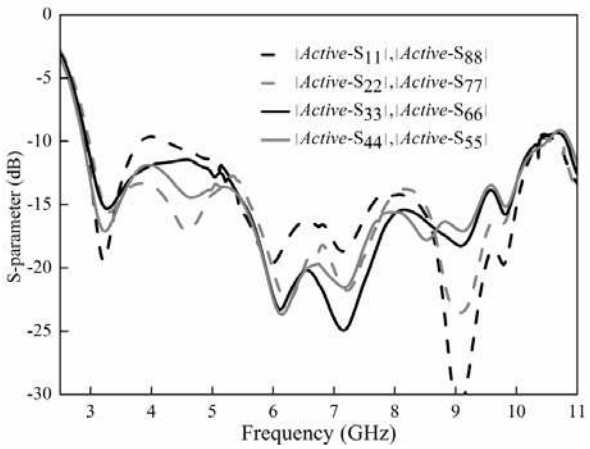

Figure 5. Simulated active-S parameters of each port for the eight-element array.

in the array are connected to each other and share a common side, the element spacing d can be kept very small and the distance is as the length of the single radiator. Therefore, d is selected as 30 mm and equals to the wavelength at 10 GHz, indicating the grating lobes can be avoided. Figure 5 presents the predicted active-S parameters for each port the eight-element array. It is noted that, when all the elements are fully excited, the lowest operating frequency of each port is slightly shifted down to lower frequencies, thus the impedance bandwidth is increased. The impedance bandwidths of all the ports can cover the desired FCC allocated UWB frequency band.

4. UWB POWER DIVIDER DESIGN

In order to achieve a compact integrated UWB antenna array and avoid requiring an external commercial feeding network, a UWB power divider is required to feed the antenna array. The single-stage Wilkinson power divider is the mostly used power divider, as it has good isolation between two output ports and impedance matching at the input port but it has only 20% fractional bandwidth [17]. Normally, wideband characteristics can be obtained by increasing the number of sections. In [12], a 3-section Wilkinson power divider was utilized to feed the tapered slot antenna array while it has a large size. In order to achieve a compact wideband power divider for UWB systems, some techniques have been proposed. A typical method is to employ multilayer broadside-coupled microstrip-slot-microstrip [18, 19], microstrip-coplanar waveguide [20] or slotline [21] approach. The multilayer power dividers have a broad bandwidth and compact size but high insertion loss of over 4.5 dB [18–21]. Moreover, they are printed on different layers of substrates which may increase the height, cost and fabrication complexity. Recently, a modified Wilkinson power divider with wideband performance has been proposed by adding open stubs [22–24]. Compared with the multilayer wideband power dividers, the modified Wilkinson power divider only use a single layer substrate while maintaining a wideband performance and occupying a compact size. Based on this operating principle, a modified Wilkinson power divider which can operate from 3 to 11 GHz is selected to compose the eight-way binary-tree feed network for the eight-element UWB antenna array.

Figure 6 shows the geometry of a modified two-way Wilkinson power divider which can provide signals with balanced amplitudes and phases from the output ports. It is printed on a 0.5 mm thick Rogers 3003 substrate and has three ports with port 1 as input port and ports 2 and 3 as output ports. All the ports are matched at a characteristics impedance of $Z_0 = 50\,\Omega$. The characteristic impedance of the shunt stub is $Z_1 = 70\,\Omega$. The length of the shunt stub is $l = 7.8$ mm which is around a quarter guided wavelength at the center frequency of the operating band. The inner distance between the two shunt stubs is $s = 1.2$ mm which is around the length of a resistor. The value of the shunt resistor is $R = 100\,\Omega$. In addition, two open-circuited stubs are attached to the shunt stubs, respectively. The arrangement is to obtain more design flexibility for achieving better performance. The characteristic

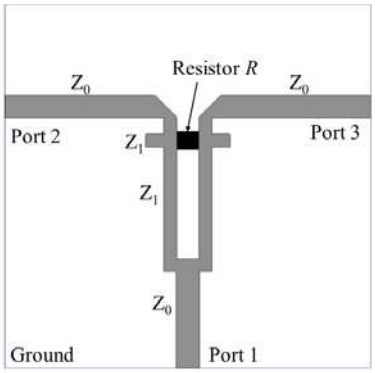

Figure 6. Geometry of a modified two-way Wilkinson power divider with stub matching.

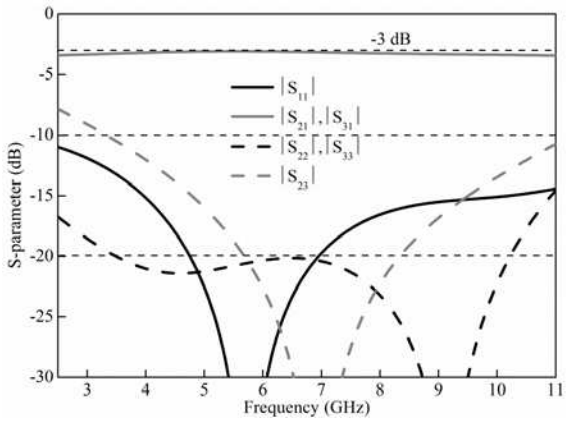

Figure 7. Simulated S-parameters of the modified two-way Wilkinson power divider.

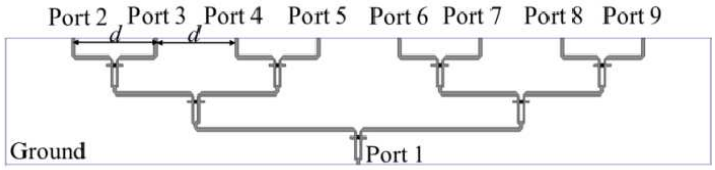

Figure 8. Geometry of the modified eight-way binary-tree Wilkinson power divider.

impedance of the open-circuited stub is the same as that of the shunt stub. The simulated S-parameters of the power divider are shown in Figure 7. As expected, the reflection coefficient of the input and output ports below -10 dB across a wide frequency range from 2.5 to 11 GHz with $|S_{11}| \leq -15$ dB from 4 to 11 GHz and $|S_{22}| \leq -20$ dB from 3.5 to 10 GHz. Moreover, the insertion loss is reduced to 3.24 dB with fluctuation of ± 0.15 dB.

In order to feed the eight-element array, the previous modified Wilkinson power divider is chosen to compose the eight-way binary-tree divider. As shown in Figure 8, the power divider has nine ports with port 1 as input port and ports 2–9 as output ports. The distance between any two adjacent outputs has the same value of d which is also the element spacing of the eight-element array.

5. INTEGRATED UWB ANTENNA ARRAY

Based on the analysis in previous sections, the integrated eight-element UWB antenna array is obtained and shown in Figure 9. The tapered baluns and the eight-way binary-tree power divider are printed on the same Rogers 3003 substrate. The antenna element and power divider of the integrated antenna array have the same dimensions as that shown in Figures 1 and 8. The integrated antenna array occupies a

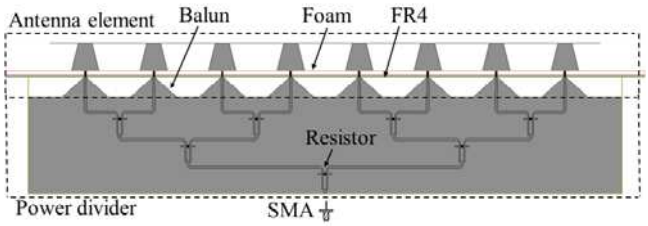

Figure 9. Geometry of the integrated eight-element array.

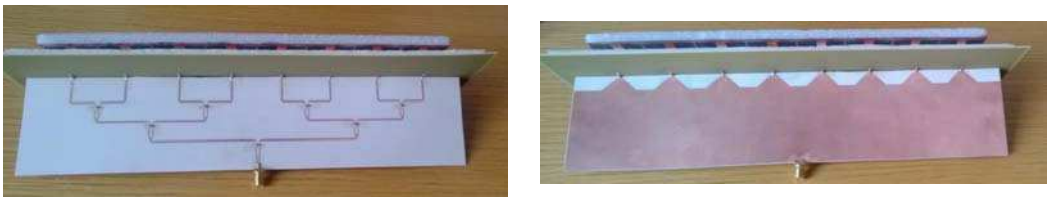

(a) (b)

Figure 10. Photo of the fabricated prototype. (a) Top view. (b) Bottom view.

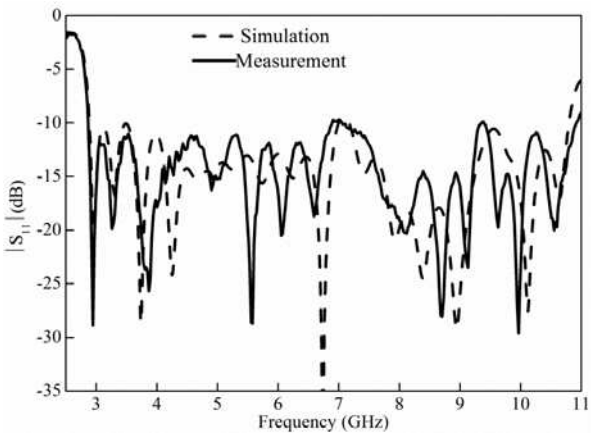

Figure 11. Simulated and measured reflection coefficient of the integrated antenna array.

Table 1. Pattern characteristics of the integrated antenna array at 3, 6 and 9 GHz.

Frequency (GHz)	F/B ratio (dB)	Boresight gain (dBi)	X. pol. level (dB)	Side lobe level (dB)
3	16	13.24	−25	−16
6	14	13.1	−17	−13
9	8	13.82	−20	−10

volume of 280 mm × 70 mm × 15 mm. In order to verify the design concept, a prototype of the array has been fabricated and tested. The photo of the prototype is shown in Figure 10.

The comparison of the reflection coefficient between simulation and measurement is shown in Figure 11. Both simulated and measured results confirm that, the impedance bandwidth of the integrated antenna array ($|S_{11}| \leq -10$ dB) is from 2.9 to 10.8 GHz or 115% which covers the desired frequency band from 3.1 to 10.6 GHz.

The measured radiation patterns of the integrated antenna array are illustrated in Figure 12. Relatively stable radiation patterns across the operating frequency range have been obtained. It is noticed that the beamwidth in the E-plane is larger than that in the H-plane. Moreover, the beamwidth in the H-plane slightly decreases against operating frequency. The pattern characteristics of the array are summarized in Table 1. The F/B ratio reduces versus frequency with 16, 14 and 8 dB at 3, 6 and 9 GHz, respectively. Low cross-polarization levels in the whole frequency band have been achieved with −25 dB at 3 GHz, −17 dB at 6 GHz and −20 dB at 9 GHz. In addition, the side lobe level slightly increases from −16 to −10 dB in terms of frequency as the electric length of the element spacing increases.

Figure 13 presents the measured antenna gain for the integrated UWB antenna array. As illustrated, relatively consistent gain performance can be observed. In the operating frequency band, the maximum boresight gain is 13.97 dBi at 8 GHz while the minimum boresight gain is 10.7 dBi at 10.5 GHz. The obtained 3-dB gain bandwidth of the integrated UWB antenna array is 110% (from 2.9 to 10 GHz).

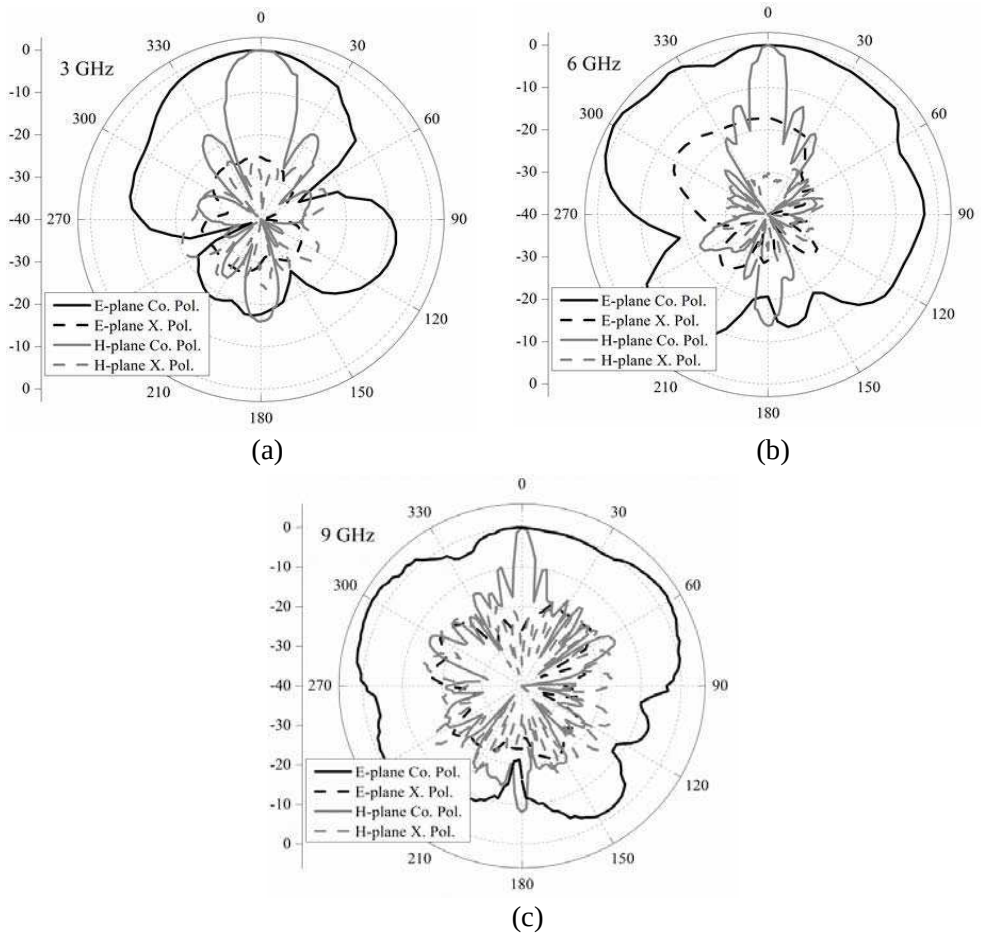

Figure 12. Measured radiation patterns in two principal planes at different frequencies. (a) 3 GHz. (b) 6 GHz. (c) 9 GHz.

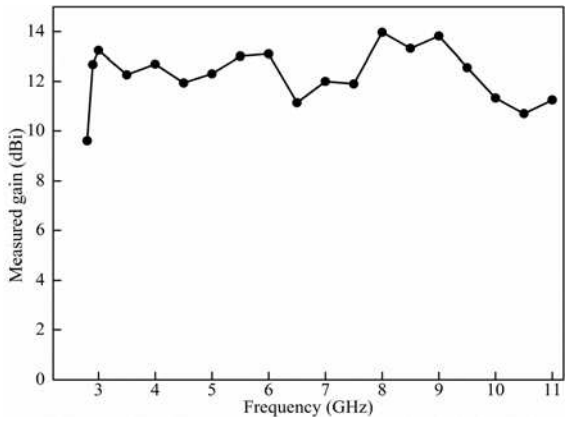

Figure 13. Measured boresight antenna gain against frequency.

6. CONCLUSION

A connected UWB antenna array has been proposed in this work. The array is formed by eight UWB antenna elements which are connected to reduce the distance and avoid grating lobe. Each antenna element comprises a slot patch and two L-shaped feeds. A tapered balun has been utilized in the

design to achieve low cross-polarization levels. To avoid using commercial feeding network, a modified Wilkinson power divider with UWB performance has been applied to excite the antenna array. Hardware realization is used to evaluate and validate the design theory. Performance of the design features wide impedance matching, directional radiation patterns and low cross-polarization level thus promising for UWB imaging radar systems.

ACKNOWLEDGMENT

The project is supported by the funding from Surrey Space Centre, University of Surrey, UK, Department of Computing, University of Surrey, UK, University of Kent, UK, China Scholarship Council, and the Fundamental Research Funds for the Central Universities of China (2014B13114). Some measurements were carried out at the anechoic chamber of the Antenna Group at University of Bradford, UK. The authors would like to thank Prof. Raed A. Abd-Alhameed and Dr. Chan See for their help during the measurement.

REFERENCES

1. Allen, B., M. Dohler, E. E. Okon, W. Q. Malik, A. K. Brown, and D. J. Edwards, *Ultra-wideband Antennas and Propagation for Communications, Radar and Imaging*, Chapter 1, 1–5, Wiley, New York, 2007.
2. Kindt, R. W., M. Kragalott, M. G. Parent, and G. C. Tavik, "Preliminary investigations of a low-cost ultrawideband array concept," *IEEE Transactions on Antennas and Propagation*, Vol. 57, No. 12, 3791–3799, 2009.
3. Godard, A., L. Desrumaux, V. Bertrand, J. Andrieu, B. Jecko, V. Couderc, M. Brishoual, and R. Guillerry, "A transient UWB antenna array used with complex impedance surfaces," *International Journal of Antennas and Propagation*, Article ID 243145, 200.
4. Desrumaux, L., A. Godard, M. Lalande, V. Bertrand, J. Andrieu, and B. Jecko, "An original antenna for transient high power UWB arrays: The Shark antenna," *IEEE Transactions on Antennas and Propagation*, Vol. 58, No. 8, 2515–2522, 2010.
5. Ito, Y., M. Ameya, M. Yamamoto, and T. Nojima, "Unidirectional UWB array antenna using leaf-shaped bowtie element and flat reflector," *Electronics Letters*, Vol. 44, No. 1, 9–11, 2008.
6. Ren, Y. J., C. P. Lai, P. H. Chen, and R. M. Narayanan, "Compact ultrawideband UHF array antenna for through-wall radar applications," *IEEE Antennas and Wireless Propagation Letters*, Vol. 8, 1302–1305, 2009.
7. Gentner, P. K., G. S. Hilton, M. A. Beach, and C. F. Mecklenbrauker, "Characterisation of ultra-wideband antenna arrays with spacings following a geometric progression," *IET Communication*, Vol. 6, No. 10, 1179–1186, 2012.
8. Sugitani, T., S. Kubota, A. Toya, X. Xiao, and T. Kikkawa, "A compact 4×4 planar UWB antenna array for 3-D breast cancer detection," *IEEE Antennas and Wireless Propagation Letters*, Vol. 12, 733–736, 2013.
9. Chamaani, S., M. S. Abrishamian, and S. A. Mirtaheri, "Time-domain design of UWB Vivaldi antenna array using multiobjective particle swarm optimization," *IEEE Antennas and Wireless Propagation Letters*, Vol. 9, 666–669, 2010.
10. Liao, C. H., P. Hsu, and D. C. Chang, "Energy patterns of UWB antenna arrays with scan capability," *IEEE Transactions on Antennas and Propagation*, Vol. 59, No. 4, 1140–1147, 2011.
11. Yao, Y., M. Liu, W. Chen, and Z. Feng, "Analysis and design of wideband widescan planar tapered slot antenna array," *IET Communication*, Vol. 4, No. 10, 1632–1638, 2010.
12. Yang, Y., Y. Wang, and A. E. Fathy, "Design of compact Vivaldi antenna arrays for UWB see through wall applications," *Progress In Electromagnetics Research*, Vol. 82, 401–418, 2008.
13. Zhu, F. G., S. Gao, A. Ho, R. A. Abd-abhameed, C. See, J. Z. Li, G. Li, and J. D. Xu, "Ultra-wideband dual-polarized patch antenna with four capacitively coupled feeds," *IEEE Transactions on Antennas and Propagation*, Vol. 62, No. 5, 2440–2449, 2014.

14. Zhang, K., F. G. Zhu, and S. Gao, "Differential-fed ultra-wideband slot-loaded patch antenna with dual orthogonal polarisation," *Electronics Letters*, Vol. 49, No. 25, 1591–1592, 2013.
15. Mehdipour, A., K. M. Aghdam, M. R. K. Khatib, and R. F. Dana, "A practical feeder for differential elliptical antennas in ultra-wideband applications," *Microwave and Optical Technology Letters*, Vol. 50, No. 8, 2103–2107, 2008.
16. Mailloux, R. J., *Phased Array Antenna Handbook*, 2nd Edition, Artech House, 2005.
17. Wilkinson, E., "An N-way hybrid power divider," *IRE Transactions on Microwave Theory and Techniques*, Vol. 8, No. 1, 116–118, 2006.
18. Abbosh, A. M., "A compact UWB three-way power divider," *IEEE Microwave and Wireless Components Letters*, Vol. 17, No. 8, 598–600, 2007.
19. Abbosh, A. M., "Design of ultra-wideband three-way arbitrary power dividers," *IEEE Transactions on Microwave Theory and Techniques*, Vol. 56, No. 1, 194–201, 2008.
20. Abbosh, A. M., "Ultra-wideband three-way power divider using broadside-coupled microstrip-coplanar waveguide," *Microwave and Optical Technology Letters*, Vol. 54, No. 1, 196–199, 2012.
21. Song, K. and Q. Xue, "Novel ultra-wideband (UWB) multilayer slotline power divider with bandpass response," *IEEE Microwave and Wireless Components Letters*, Vol. 20, No. 1, 13–15, 2010.
22. Zhou, B., H. Wang, and W. X. Sheng, "A modified UWB Wilkinson power divider using delta stub," *Progress In Electromagnetics Research Letters*, Vol. 19, 49–55, 2010.
23. Ahmed, O. and A. R. Sebak, "A modified Wilkinson power divider/combiner for ultrawideband communications," *2009 IEEE Antennas and Propagation Society International Symposium*, 1–4, Charleston, 2009.
24. Wong, S. W. and L. Zhu, "Ultra-wideband power divider with good in-band splitting and isolation performances," *IEEE Microwave and Wireless Components Letters*, Vol. 18, No. 8, 518–520, 2008.